

FIG. 3. PCRM (ξ) and PRM $\{[R(R+1)]^{1/2}\}$ angular momenta corresponding to the wave functions of Fig. 2.

family of states pertaining to a definite signature²) the ξ values first increase in an approximately monotonic way. In the PRM case the motion of the rotor is described in a fully quantal manner. \vec{R} is a vector operator, free to move in the plane perpendicular to the 3 axis, and R^2 has a spectrum of eigenvalues restricted to even integers and its quantal nature is especially important at low spin values. For total spin values near $\frac{13}{2}$, the tendency of the system is to try to minimize the rotational energy since $\vec{R} = \vec{I} - \vec{J}$. On the other hand, the angular velocity is a classical vector directed along the 1 axis in the PCRM just restricted by the constraint (6) which allows ω to take smaller values thus giving purer wave functions. Both models become equivalent as fluctuations become more unimportant.

To summarize, the PRM is shown to provide a fair reproduction of strongly Coriolis-distorted bands in the deformed rare-earth region. The need of introducing *ad hoc* attenuation factors appears to stem from the neglect of the recoil term in the PRM Hamiltonian. The latter transforms the conventionally called Coriolis interaction $-\hbar^2 \times (\vec{I}^\perp \cdot \vec{J}^\perp) / \theta$ into the true one $-\hbar \vec{J} \cdot \vec{\omega}$. While the Nilsson model describes an independent-particle picture in the intrinsic reference frame, the recoil term brings in an aspect of the many-body problem through the moment of inertia of the core. The recoil term cannot be absorbed into the mean field in a universal form and thus has to be considered explicitly.

Stimulating discussions with Professor D. Bès, Professor H. J. Mang, Professor M. A. J. Mariscotti, and Professor P. Ring are gratefully acknowledged.

¹S. A. Hjorth and W. Klamra, Z. Phys. **A283**, 287 (1977), and references therein.

²A. Bohr and B. R. Mottelson, *Nuclear Structure* (Benjamin, New York, 1975), Vol. 2.

³P. Ring and H. J. Mang, Phys. Rev. Lett. **33**, 1174 (1974).

⁴P. Ring, M. J. Mang, and B. Banerjee, Nucl. Phys. **A25**, 141 (1974).

⁵E. Osnes, J. Rekstad, and O. K. Gjøtterud, Nucl. Phys. **A253**, 45 (1975).

⁶P. H. Stelson and L. Grodzins, Nucl. Data **A1**, 21 (1965).

⁷J. P. Davidson, *Collective Models of the Nucleus* (Academic, New York, 1968), p. 183.

Influence of Retardation on the Angular Distribution of Radiative Electron Capture

E. Spindler, H.-D. Betz, and F. Bell

Sektion Physik, Universität München, 8046 Garching, Germany

(Received 5 February 1979)

Angular distributions and forward-backward intensities of photons emitted during electron capture have been measured in collisions between fast projectile ions (93-MeV oxygen, 110–123-MeV sulfur) and target atoms. In contrast to previous expectations, the radiation pattern in the laboratory system is not strongly shifted in forward direction but turned out to exhibit forward-backward symmetry independent of the projectile velocity. We attribute these findings to a cancellation between the Doppler-shift and retardation effects.

Radiative electron capture (REC) is a collision process in which an ion captures an electron and emits a photon. REC of free electrons has been

known for a long time, mainly from work in astrophysics and plasma physics where it is an important recombination process. More recently,

REC of bound target electrons has been identified in heavy-ion-atom collisions¹ and has been studied since in numerous contributions. Some basic REC features, such as total cross sections in simple collision systems, have been treated theoretically^{2,3} and experimental line profiles of the emitted radiation have been analyzed in detail.^{4,5}

REC of free electrons can be considered as the inverse photoeffect; for this reason, well-developed formalisms are already available and, according to the principle of detailed balance, the differential cross section for REC, $d\sigma_{\text{REC}}/d\Omega_{\text{ph}}$, is proportional to the differential cross section for the photoeffect, $d\sigma_{\text{PE}}/d\Omega_{\text{el}}$, where $d\Omega_{\text{ph}}$ and $d\Omega_{\text{el}}$ represent solid angles for photons and electrons in the reference frame of the atom and ion, respectively. As a consequence, the angular distribution of REC can be derived from the one for the photoeffect. When retardation is neglected, i.e., when the factor $\exp(i\vec{k}\cdot\vec{r})$ in the matrix element for the radiative transition process is omitted, one obtains for REC into $1s$ orbitals a symmetric distribution $I_{\text{REC}}(\vartheta_{\text{ion}}) \propto \sin^2\vartheta_{\text{ion}}$. Here, $\vartheta_{\text{ion}} = \pi - \varphi_{\text{ion}}$, where φ_{ion} denotes the angle between the photon and electron velocities for both the photoeffect and REC in the emitting system. We emphasize, though, that the $\sin^2\vartheta_{\text{ion}}$ term is not strictly valid when *target* electrons are captured compared to completely *free* electrons; in the first case, transverse momenta occur which give rise to an intensity enhancement especially at small forward and backward angles.⁴ Since the ion system moves with a velocity v relative to the laboratory frame, a Lorentz transformation can be applied,

$$\cos\vartheta_{\text{ion}} = \frac{-\beta + \cos\vartheta_{\text{lab}}}{1 - \beta \cos\vartheta_{\text{lab}}}, \quad (1)$$

$$\frac{d\Omega_{\text{ion}}}{d\Omega_{\text{lab}}} = \frac{1 - \beta^2}{(1 - \beta \cos\vartheta_{\text{lab}})^2},$$

and yields the observable asymmetric, forward-shifted distribution⁶

$$I_{\text{REC}}(\vartheta_{\text{lab}}) \propto \sin^2\vartheta_{\text{lab}} / (1 - \beta \cos\vartheta_{\text{lab}})^4, \quad (2)$$

where $\beta = v/c$ and ϑ_{lab} stands for the angle between beam direction and detected REC photon. More refined theoretical treatments of the angular distribution for REC radiation have not been available.

An early investigation of experimental REC distributions with fast sulfur ions did not give good agreement of forward-backward intensities from measurement and Eq. (2).⁶ However, further ex-

perimental studies by other authors^{7,8} were claimed to reveal no discrepancies with theory as outlined above. In order to clarify the situation, a more careful examination of the angular distribution was undertaken.

Oxygen and sulfur ions with energies between 93 and 123 MeV were obtained from the Munich Tandem Van de Graaff accelerator and were directed onto beryllium, carbon, and aluminum targets with thicknesses between 60 and 260 $\mu\text{g}/\text{cm}^2$. In one experiment, a Si(Li) x-ray detector was used to observe the radiation due to REC into the K shell of the ions, peaked at energies near 5 keV in case of sulfur ions, and could be moved to angles ranging from 8° to 135° . In a second experiment, three x-ray detectors were mounted at fixed angles of 30° , 90° , and 150° with respect to the beam axis. In all sulfur experiments, carbon absorbers were used to reduce the count rate due to characteristic sulfur K lines; in the oxygen runs, no additional absorber was required for C targets. All absorbers used were carefully calibrated in order to allow an accurate channel-by-channel correction of counts in the energy range where REC is of interest. Rutherford scattering and integration of beam current, together with measurement of solid angles of the x-ray detectors and excitation of highly isotropic target K x-ray lines ($\text{Cu } K\alpha$), were employed to obtain absolute cross sections and properly normalized angular distributions. Sample spectra of REC distributions in the system S-C are shown in Fig. 1.

Determination of REC intensities for the various observation angles is straightforward. Absorber corrections were applied channel by channel; at the peak intensity, correction factors did not exceed ~ 2 . Then, counts between fixed photon-energy windows were integrated. These windows were moved in spectra for different observation angles according to the Doppler shift of the measured radiation. The easily observable shifts of the REC peaks as a function of ϑ_{lab} give clear evidence that the velocity of the emitting system is precisely the beam velocity and that Doppler shifts must be performed with the full relative velocity between target atoms and projectile ions. Figure 1 shows that especially at high radiation energies a certain additional background radiation must be assumed which is not explained by our theoretical REC line profiles. This background may originate in bremsstrahlung of secondary electrons and in radiation due to combined-atom effects. Fortunately, the intensity of this

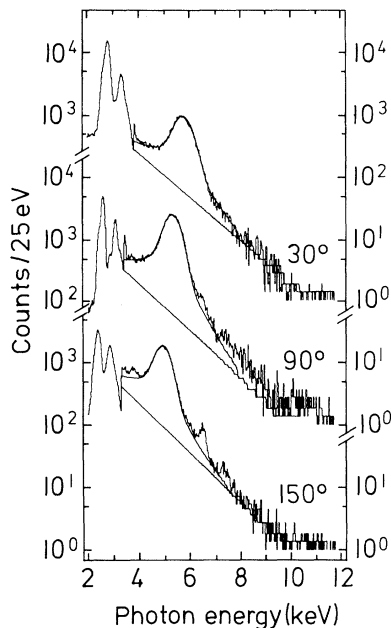


FIG. 1. Experimental REC spectra (histograms) from collisions between 123-MeV sulfur and 260- $\mu\text{g}/\text{cm}^2$ carbon for three observation angles. Absorber corrections are applied for photon energies above ~ 3.5 keV. Also shown are theoretical REC line profiles (Refs. 4 and 5) and remaining exponential background.

background is small and, for sulfur ions, amounts to no more than $\sim 10\%$ of the total REC intensity and, thus, does not critically affect the present REC analysis.

We found that total REC intensities observed at symmetric forward-backward angles did not differ from each other outside experimental uncertainties of $\sim 10\%$. Table I summarizes our results. In all cases investigated we found no for-

TABLE I. Forward-backward intensity ratios of REC radiation in various collision systems. Target thicknesses are given parenthetically in $\mu\text{g}/\text{cm}^2$; all targets were oriented at 45° with respect to the beam direction. Experimental ratios (column 4) are close to unity as is predicted by Eq. (4), but disagree with values derived from Eq. (2) (without retardation).

$\vartheta_{\text{lab}}/\vartheta_{\text{lab}'}$	Projectile	Target	$I(\vartheta_{\text{lab}})/I(\vartheta_{\text{lab}'})$	
			Expt.	Eq. (2)
30°/150°	93-MeV O	C (260)	1.07 ± 0.2	2.17
30°/150°	123-MeV S	C (145)	0.98 ± 0.1	1.88
30°/150°	123-MeV S	C (260)	0.99 ± 0.1	1.88
30°/150°	123-MeV S	Al (200)	1.03 ± 0.15	1.88
45°/135°	110-MeV S	C (60)	0.98 ± 0.1	1.63

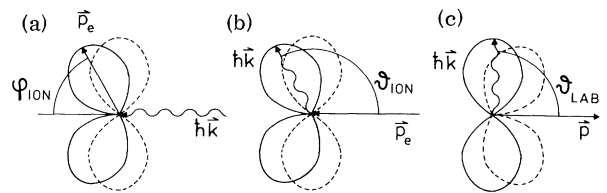


FIG. 2. Schematic illustration of the angular distribution of photoeffect (a) and REC in the emitting system (b) and in the laboratory system (c). Full and dashed lines refer to distributions with and without retardation, respectively; $\hbar\vec{k}$ and \vec{p}_e refer to the momentum of photon and electron, and \vec{p} stands for the momentum of a moving ion in the laboratory system.

ward-backward asymmetry, though Eq. (2) predicts such asymmetries which, in the present cases, would have been as large as a factor of ~ 2 .

We attribute these findings to retardation effects. In the case of the photoeffect, retardation is not necessarily a small correction; in the non-relativistic limit one obtains⁹

$$I_{\text{PE}}(\varphi_{\text{ion}}) \propto \sin^2 \varphi_{\text{ion}} (1 - \beta \cos \varphi_{\text{ion}})^{-4}. \quad (3)$$

In order to derive the corresponding REC distribution corrected for retardation, we apply a Lorentz transformation to the laboratory system according to Eq. (1); this procedure yields the final angular distribution

$$I_{\text{REC}}(\vartheta_{\text{lab}}) \propto \sin^2 \vartheta_{\text{lab}}. \quad (4)$$

Thus the backward shift of the REC distribution in the projectile system relative to the direction of projectile motion, caused by retardation, is canceled by the forward shift due to Doppler transformation (Fig. 2), and forward-backward symmetry is established as observed experimentally. To our knowledge, it has not been noted before that retardation and Doppler transformations cancel each other in collision systems such as the present ones. It should be noted that this cancellation occurs only when the velocity \vec{v}_r , which causes retardation equals the velocity $-\vec{v}$ which determines the Doppler transformation. However, since target electrons are not at rest and exhibit an intrinsic velocity distribution, the relevant values of \vec{v}_r are distributed around \vec{v} and, thus, give rise to some distortion of the forward-backward symmetry of REC radiation. We argue that this effect becomes important only for small forward and backward angles and does not significantly affect the present data and their interpretation.

In a relativistic treatment of the photoeffect based on the Born approximation and hydrogenic Dirac functions, Sauter¹⁰ derived an angular distribution for K electrons which can be used to replace Eq. (3) and, after performance of the transformation outlined above, gives a REC distribution for highly relativistic collisions,

$$I_{\text{REC,rel}}(\vartheta_{\text{lab}}) \propto \sin^2 \vartheta_{\text{lab}} \left[1 + \frac{(\gamma-1)(\gamma-2)}{2\gamma(1-\beta \cos \vartheta_{\text{lab}})} \right], \quad (5)$$

where $\gamma = (1-\beta^2)^{-1/2}$. It is interesting to note that $I_{\text{REC,rel}}(\vartheta_{\text{lab}})$ remains quite symmetric with respect to forward-backward intensities even for very high collision velocities. Since deviations from such a symmetry are relatively easy to measure, the possibility may arrive to check relativistic angular distributions for the photoeffect by means of REC measurements.

In conclusion, we have shown that retardation effects are very important in a discussion of REC and can be measured quantitatively. In particular, shifts of the angular distribution due to retardation are offset by the Doppler effect. Among further consequences of the presented results, we point out that retardation effects may become important in connection with the observation of angular distributions of other collision-induced radiation phenomena such as, for example, combined-atom x-ray continua resulting from either REC into molecular orbitals¹¹ or, perhaps, transitions between quasimolecular orbitals.

We acknowledge discussions with M. Kleber and Č. Zupančič. This work was supported in part by

the Bundesministerium für Forschung und Technologie.

¹H. W. Schnopper, H.-D. Betz, J. P. Delvaille, K. Kalata, A. R. Sohval, K. W. Jones, and H. E. Wagner, *Phys. Rev. Lett.* **29**, 898 (1972).

²M. Kleber and D. H. Jakubassa, *Nucl. Phys. A* **252**, 152 (1975).

³J. S. Briggs and K. Dettmann, *J. Phys. B* **10**, 1113 (1977).

⁴H.-D. Betz, M. Kleber, E. Spindler, F. Bell, H. Panke, and W. Stechling, in *Proceedings of the Ninth International Conference on the Physics of Atomic and Electronic Collisions*, edited by J. S. Risley and R. Geballe (Univ. Washington Press, Seattle, 1975), p. 520.

⁵E. Spindler, H.-D. Betz, and F. Bell, *J. Phys. B* **10**, L561 (1977).

⁶H.-D. Betz, F. Bell, H. Panke, and G. Kalkoffen, in *Proceedings of the Fourth International Conference on Atomic Physics. Abstracts of Contributed Papers, Heidelberg, Germany, 1974*, edited by J. Kowalski and H. G. Weber, (Heidelberg Univ. Press, Heidelberg, Germany, 1974), p. 670.

⁷J. Lindskog, J. Phil, R. Sjödin, A. Marelus, K. Sharma, R. Hallin and P. Lindner, *Phys. Scr.* **14**, 100 (1976).

⁸R. Schulé, H. Schmidt-Böcking, and I. Tserruya, *J. Phys. B* **10**, 889 (1977).

⁹H. A. Bethe and E. E. Salpeter, in *Handbuch der Physik*, edited by S. Flügge (Springer, Berlin, 1957), p. 397.

¹⁰F. Sauter, *Ann. Phys. (Leipzig)* **11**, 454 (1931), and **9**, 217 (1931).

¹¹W. Wölfli, Ch. Stoller, G. Bonani, M. Stöckli, M. Suter, and W. Däppen, *Z. Phys. A* **286**, 249 (1978).

Interactions of Blackbody Radiation with Atoms

T. F. Gallagher and W. E. Cooke

Molecular Physics Laboratory, SRI International, Menlo Park, California 94025

(Received 19 December 1978)

Blackbody radiation affects low-frequency ($h\nu \ll kT$) atomic transitions both by inducing transitions and producing ac frequency shifts, important effects that have previously been ignored. Here we report the calculation and experimental observation of a manifestation of the former, the threefold reduction of the Na np radiative lifetimes by 300-K blackbody-radiation-induced stimulated emission and absorption. Estimates of ac frequency shifts for Rydberg and ground-state atoms are given.

In most cases the effects of room-temperature blackbody radiation on atomic systems are ignored, and justifiably so. However, the thermal bath of blackbody photons can be quite important for low-frequency ($h\nu \ll kT$) transitions in an

atom because it both induces transitions and produces ac Stark or Zeeman shifts. These effects are most dramatic for atoms in highly excited or Rydberg states because these states have low-frequency transitions with enormous electric di-